Eastern Region Technical Attachment
No. 2019-01
March 2019

Convection Along Southern ZDC Surface Boundaries During Forecast Low Probability Severe Weather Avoidance Plan Days

Sean T. Campbell
NOAA/National Weather Service
Leesburg, Virginia

Abstract

Widespread afternoon and evening convection across the southern half of Washington Air Route Traffic Control Center's (ZDC's) airspace negatively impacts air traffic flow to and from the Caribbean and several of the busiest airports in the southeastern United States, including Hartsfield-Jackson Atlanta International Airport, Charlotte Douglas International Airport, Orlando International Airport and Miami International Airport. To avoid the convection, the Federal Aviation Administration may implement a Severe Weather Avoidance Plan (SWAP). On 30 days from April to October of 2015, 2016 and 2017, when a low probability (less than a 50% chance) of a SWAP was forecast by ZDC Center Weather Service Unit meteorologists, surface boundaries across the southern half of ZDC helped provide the focus for convection that resulted in a SWAP. This technical attachment describes and discusses different types of surface boundaries across the southern half of ZDC along which SWAP-causing convection developed and propagated on those 30 days. Also highlighted are other environmental factors that worked in concert with the surface boundaries to generate and maintain the convection.

**Corresponding author address*: Sean Campbell, NOAA/National Weather Service/Washington CWSU, 825 E. Market St, Leesburg, VA 20176. E-mail: sean.campbell@noaa.gov

1. Introduction

When under-forecast convection occurs across the southern half of Washington Air Route Traffic Control Center's (ZDC's) airspace, the Federal Aviation Administration (FAA) may implement an unexpected Severe Weather Avoidance Plan (SWAP). Air traffic management initiatives resulting from the SWAP disrupt the flow of air traffic across the eastern United States, particularly during the afternoon and evening, when air traffic volume is high. Such was the case on 30 days during the April to October timeframe of 2015, 2016 and 2017 when a low probability of a SWAP was forecast across the southern half of ZDC (SHZDC) – Fig. 1. SWAP actions included jet route closures and re-routing of aircraft to avoid convection across SHZDC, impacting air traffic flowing to and from the Caribbean and busy southeastern United States airports including Hartsfield-Jackson Atlanta International Airport, Charlotte Douglas International Airport, Orlando International Airport and Miami International Airport.

To alert National Airspace System (NAS) planners and the ZDC Supervisory Traffic Management Coordinator of the potential for convectively-caused SWAP, ZDC National Weather Service (NWS) Center Weather Service Unit (CWSU) meteorologists issue SWAP forecast statements by 1430 UTC each morning from April through October. These probability-based forecasts are valid from issuance to an end time that is situationally dependent, but usually ranges from the late evening to the middle of the night (0200 UTC to 0500 UTC). Using criteria established by Squires and Struckmann (2009), SWAP probabilities include "SWAP Expected" (chance of SWAP is equal to or greater than 95%), "SWAP Probable" (chance of SWAP is between 50% and less than 95%), "SWAP Possible" (chance of SWAP is greater than 0% and less than 50%) and "SWAP Not Expected" (chance of SWAP is 0%). Additionally, SWAP forecast statements also contain a brief synopsis that includes important information such as when and where convection may develop and move, the extent of convective coverage, maximum height of convective tops and which jet routes, airports and airport arrival/departure gates within ZDC may be impacted.

One of the primary factors that helped "tipped the scales" in favor of widespread convection across SHZDC on the 30 under-forecast SWAP days in this study was the presence of at least one synoptic-scale frontal boundary across SHZDC. Two types of these synoptic-scale boundaries were categorized, but mesoscale surface boundaries such as sea-breeze fronts, Piedmont Troughs (PTs) and convection-generated outflow boundaries also influenced convective development and evolution. The importance of these surface boundaries and other environmental factors on convection that led to the SWAPs across SHZDC is the focus of this technical attachment (TA).

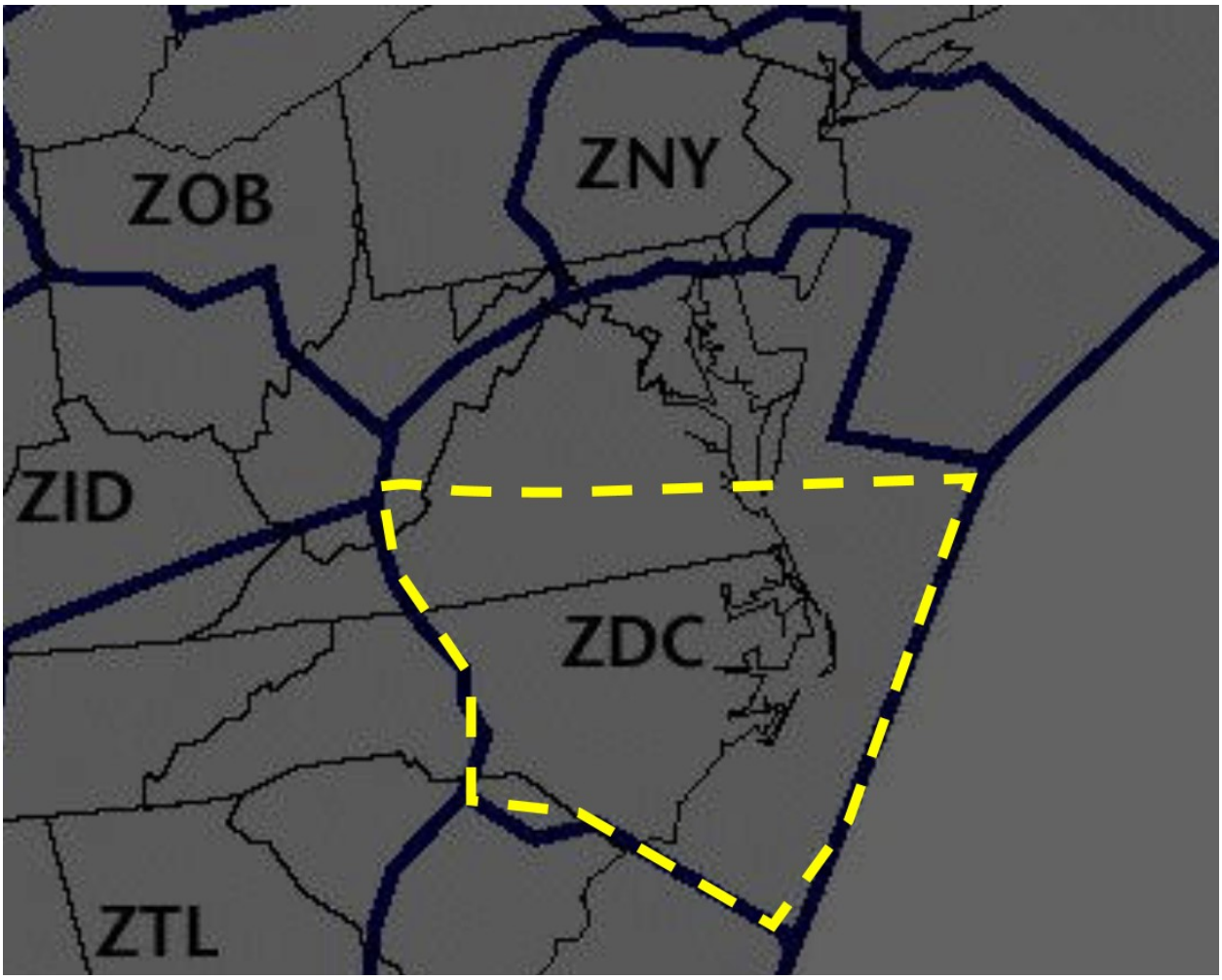

Figure 1. ZDC airspace, with a yellow dashed line delineating the study area. Map courtesy of the FAA.

2. Data and Methodology

SWAP impacts were gathered from daily FAA Northeast Recap logs. After collecting the impacts, data contained in the logs were analyzed and compared to time-stepped NWS Storm Prediction Center (SPC) Hourly Mesoscale Analysis Archive (HMAA: http://www.spc.noaa.gov/exper/ma_archive/) products and archived radar/satellite images from the Iowa Environmental Mesonet (IEM: http://mesonet.agron.iastate.edu/GIS/apps/rview/warnings.phtml) to determine times, locations and movement of the convection that caused SHZDC SWAPs.

Examination of NWS Weather Prediction Center (WPC) analyzed 3-hr North American surface charts (http://www.wpc.ncep.noaa.gov/archives/web_pages/sfc/sfc_archive.php), time-stepped NWS SPC HMAA surface charts and Earth Science Research Laboratory (ESRL) 6-hr National Center for Environmental Prediction (NCEP)/National Center for Atmospheric Research (NCAR) Reanalysis Data Composites (https://www.esrl.noaa.gov/psd/data/composites/hr/) revealed the surface frontal boundaries. On 29 of the 30 forecast low probability SWAP days (97%), WPC 3-hr North American surface charts depicted a

surface frontal boundary or a surface trough (or both) across SHZDC.

Data from the 12 UTC run of Localized Aviation MOS (Model Output Statistics) Program (LAMP) 1-hr and 2-hr convection forecasts (https://sats.nws.noaa.gov/~glmp/conv_arc/index.php) were compared with IEM radar/satellite data to determine the accuracy/usability of LAMP convection forecasts prior to each SWAP event discussed here. The LAMP's 12 UTC run was selected as it is the latest run available for use by ZDC CWSU meteorologists prior to issuing the SWAP forecast. It is also used by aviation meteorologists to help collaborate the 14 UTC Traffic Flow Management Convective Forecast (TCF), which is used by NAS planners to begin coordinating potential convective-related traffic management initiatives during the afternoon/evening hours. A minimum LAMP convection probability of 30% was employed during this study as this threshold has been found by the author to be useful in determining areas prone to convection that may result in a SWAP.

3. Analysis and Discussion

a. Effects of the Appalachians

The southern Appalachians may block or slow the progression of cold fronts for several hours, resulting in an increase in the cross-frontal/cross-mountain pressure gradient, eventually forcing cold air to surge across the southern Appalachians. When this occurs, a frontal zone with three different airstreams may form, with north-northwesterly flow surging over the Appalachians into the Carolinas, west-southwesterly flow around the southern Appalachians and southerly flow in the eastern/central Carolinas all converging in the western/central Carolinas (O'Handley and Bosart 1996, see their Figure 5). Additionally, geostrophic adjustment forces associated with jet streaks and short-wave troughs moving over a mountain range (in this case, the Appalachians) can increase low-level convergence in the lee of the mountains (Mattocks and Bleck 1986, see their Figure 2), generating a lee low.

In some cases, the collision of airstreams around the southern Appalachians as described above may result in the formation of a lee low (O'Handley and Bosart 1996). Such a scenario tends to occur most often during the cold season, when cold fronts and cold air surges are strong, but it also materializes, albeit less frequently, with weaker cold fronts throughout the warm season. Koch and Ray (1997) note that during the warm season the frequency of lee low development tends to maximize during the afternoon/early evening, when surface heating is at its most intense. The increased low-level convergence resulting from the aforementioned mountain-influenced processes can enhance the potential for convection, especially when interacting with a nearby low-level boundary.

b. Surface boundary types

Two types of synoptic-scale surface boundaries helped focus convective development widespread enough to cause a SWAP across SHZDC during the low probability SWAP forecast days in this study. The first – Type A – consisted of both surface cold fronts (with or without pre-frontal surface troughs) moving into/across SHZDC (Fig. 2a) from a northerly direction and west to east-oriented quasi-stationary fronts along which a surface wave or area of low pressure developed and tracked eastward,

forcing part of the front southward. The second – Type B – encompassed weak/decaying quasi-stationary surface frontal boundaries that stretched from beyond ZDC boundaries eastward or southeastward into southeastern Virginia and eastern North Carolina (Fig. 2b). Table 1 lists all days (in UTC) included in this study.

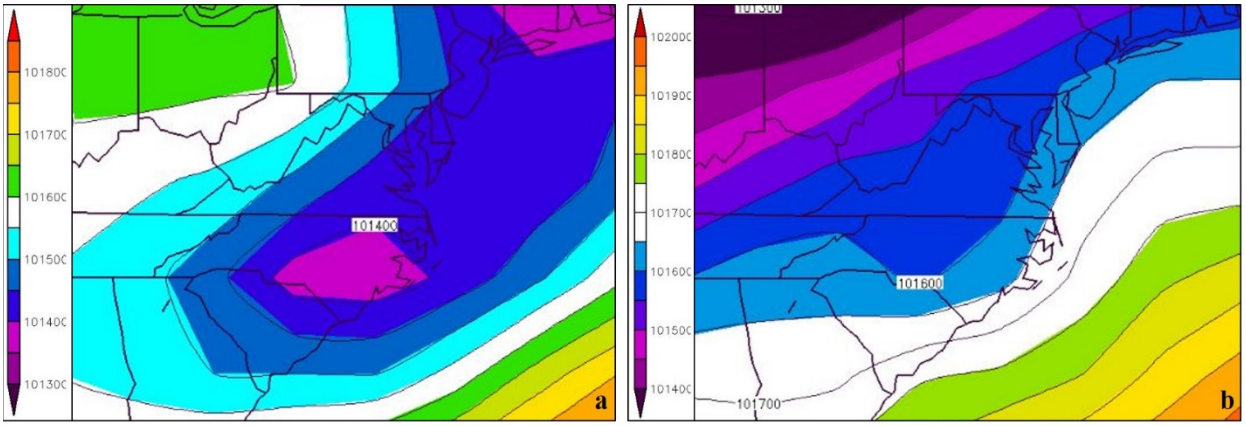

Figure 2. (a) Six-hour NCEP/NCAR reanalysis data composite images of surface sea level pressure at 18 UTC for all Type A and (b) Type B surface boundaries included in this study. Data are courtesy of NOAA/ESRL.

Table 1. All dates (UTC) when a low probability of a SWAP was forecast during which Type A or Type B surface boundaries aided in convective development and organization across SHZDC, leading to a SWAP within ZDC's airspace.

Type A surface boundary SWAP dates	Type B surface boundary SWAP dates
14 April 2015	18-19 June 2015
4-5 June 2015	25-26 June 2015
9-10 June 2015	19-20 July 2015
17-18 June 2015	8 September 2015
24-25 June 2015	29-30 May 2017
31 July-1 August 2015	31 May-1 June 2017
5-6 August 2015	4-5 June 2017
7-8 August 2015	4 July 2017
30 September-1 October 2015	19 July 2017
14-15 June 2016	6 August 2017
17-18 June 2016	14-15 August 2017
25 June 2016	2 September 2017
29-30 June 2016	
11-12 May 2017	
22-23 May 2017	
1 June 2017	
7-8 July 2017	
31 August-1 September 2017	

Synoptic-scale cold fronts often provide the impetus for convective initiation and development. During the warm season, many cold fronts crossing through SHZDC tend to lose upper-level dynamical support and weaken, becoming quasi-stationary. Some of these quasi-stationary boundaries become difficult to locate, even using surface observations, radar and satellite data. At times these quasi-stationary surface boundaries can only be detected by a weak discontinuity in a temperature or moisture gradient; they may or may not be accompanied by a weak wind shift (Koch and Ray 1997). A surface theta-e (θ_e) field (or gradient) may help to identify these boundaries (Vescio et al. 1993). However, as insignificant as these surface boundaries appear, they remain important as convection may develop/propagate along them, especially when interacting with other smaller-scale surface boundaries, mid-level short-wave troughs and/or upper-level jet maxima/divergence. Development and evolution of both isolated and lines of strong to severe convection along such surface boundaries in southern Virginia and North Carolina is well-documented (Vescio et al. 1993; Cobb 1995; Koch and Ray 1997; Pfaff 2002 and Weiss 2014).

An important mesoscale surface boundary that forms along the Carolina coastline during the warm season is the sea-breeze front. Convergence along the sea-breeze front may be strong enough to produce convection by itself when the atmosphere is moist and unstable. In Koch and Ray's (1997) study, a few sea-breeze fronts moved west or northwestward over 150 km from the Carolina coastline. This type of west-northwestward progression during the hottest part of the day may also increase the potential for convection, especially when a sea-breeze boundary collides with a Type A or Type B surface boundary.

The PT is another type of mesoscale surface boundary that influences convective development during the warm season across SHZDC. It forms near the interface of the Piedmont and coastal plain regions (Fig. 3), driven largely by differential heating due to a difference in soil types. Stronger PTs may be detectable by satellite and radar, but weaker PTs can be difficult to spot, even in 1- or 2-hPa surface analysis. PTs may also initiate convection by themselves; a case analyzed by Koch and Ray (1997) showed that clear air radar detection of a weak PT provided over 1.5 hours of lead time before the first convective cells initiated along the boundary.

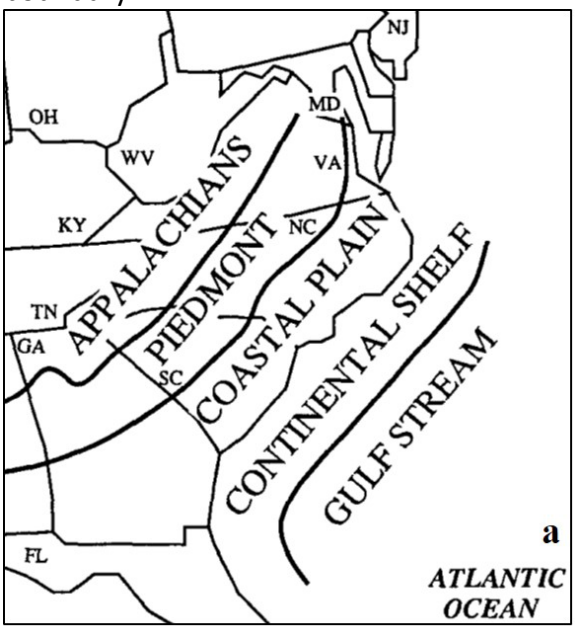

Figure 3. Topography of the southeastern United States (adapted from Dirks et al. 1988).

c. Type A surface boundaries

Type A surface boundaries comprised both surface cold fronts moving in a southward direction into or across SHZDC (Figs. 4a,b)

and west to east-oriented quasi-stationary fronts across SHZDC along which a surface wave or area of low pressure developed and tracked eastward, forcing part of the front southward. Of the 30 SWAP days included in this study, convection developed near or along Type A surface boundaries on 18 days. Sea-breeze boundaries (present on 13 Type A boundary-influenced SWAP days) and PTs (observed on 9 Type A boundary-influenced SWAP days) also helped to increase convection, especially when interacting with the Type A surface boundaries and other smaller-scale convectively-generated boundaries. Lee lows, hints of which can be seen in the surface vector wind (Fig. 4b), also helped enhance convection on 6 of the 18 Type A boundary-influenced SWAP days. Most lee lows were relatively short-lived and developed in the northeastern Georgia – western North Carolina region. Additionally, surface frontogenesis was observed where convection initiated on 17 of the 18 days when Type A boundaries enhanced convection.

Instability was important, as indicated by surface-based convective available potential energy (SBCAPE) values of at least 1000 kg m^{-2} on 17 Type A boundary-enhanced SWAP days. Effective bulk shear (EBS) values of 25 kts or greater were observed on 14 Type A boundary-enhanced SWAP days, which helped increase the potential for convection organization (Thompson et al. 2003). However, not all convection propagated in the direction of the EBS vectors. Along and ahead of Type A boundaries, θ_e ridging may help partially account for the convective precipitation pattern (Fig. 4c), including where the most intense convective activity occurred, as surface θ_e values of at least 340-348 K were observed on 16 days. During the two Type A boundary-influenced afternoons/evenings when θ_e values did not reach 340 K, convection developed within surface θ_e gradients.

Convection developed underneath areas of 300 hPa divergence during all 18 Type A boundary-influenced SWAP days. On 9 of those days, convection initiated along Type A surface boundaries below the right entrance region of a 300 hPa jet maximum, while convection developed along surface boundaries beneath the left exit region of a 300 hPa jet maximum (Rose et al. 2004) on 6 of the 18 Type A boundary-influenced SWAP days. Finally, though some were weak, transient mid-level short-wave troughs were detected prior to and during convective initiation on all 18 Type A-influenced SWAP days. These short-wave troughs also appeared to interact with both the aforementioned upper-level dynamics and surface boundaries to trigger or invigorate convection that propagated along/ahead of the Type A surface boundaries.

A review of 12 UTC LAMP convection probability forecasts revealed that using a minimum value of 30% may have increased forecaster confidence on 14 of the 18 (78% of) Type A boundary-enhanced SWAP days. During those 14 days, the LAMP 30% convection probability threshold was reached within 1-2 hours of observed convective initiation, then crossed below that threshold within 1-2 hours of observed convective dissipation. Areal coverage was generally good throughout the 14 useful LAMP convection probability forecasts, but there were times when the areal extent was off by more than 50 miles in at least one direction when compared to where convection formed/tracked. This may be, in part, a result of the 2-hour valid times of the LAMP convection products employed in this study.

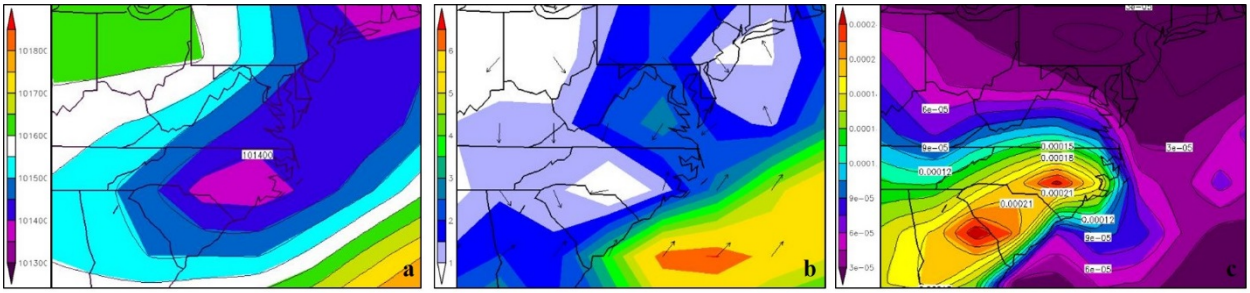

Figure 4. (a) Six-hour NCEP/NCAR reanalysis data composite images of surface sea level pressure in Pa valid at 18 UTC, (b) surface vector wind at 18 UTC, and (c) surface convective precipitation rate in mm per day averaged from 18 UTC to 00 UTC for all Type A-enhanced SWAP days in this study. Data are courtesy of NOAA/ESRL.

d. Type A surface boundaries example: 29-30 June 2016

Convection initiated shortly after 17 UTC in western North Carolina on 29 June 2016 ahead of a Type A cold front, then organized into clusters and line segments as they moved eastward, finally moving offshore of North Carolina after 06 UTC on 30 June 2016. Per FAA Northeast Recap logs, all major jet routes across SHZDC were impacted by the convection from 23 UTC on 29 June 2016 to 03 UTC on 30 June 2016. The SWAP included structured routing and re-routing to avoid the convection. Figure 5 shows a "snapshot" at 23 UTC on 29 June 2016 of the Type A boundary-enhanced convective SWAP event. Convection intensified under the right entrance region (Fig. 5a) of an upper-level jet maximum (Rose et al. 2004), with EBS vector values of 30 to 40 kts and trajectories generally from west to east (Fig. 5b). SBCAPE values were 1000-2000 J kg^{-2} (Fig. 5c). Low-level moisture was present, as surface θ_e values were within the 340-352 K range (Fig. 5d); areas of weak surface frontogenesis existed across central/western North Carolina (Fig. 5e). By 23 UTC on 29 June 2016, convection had organized into small clusters and line segments, with anvil cirrus extending over 100 km east-northeast from parent convection (Fig. 5f).

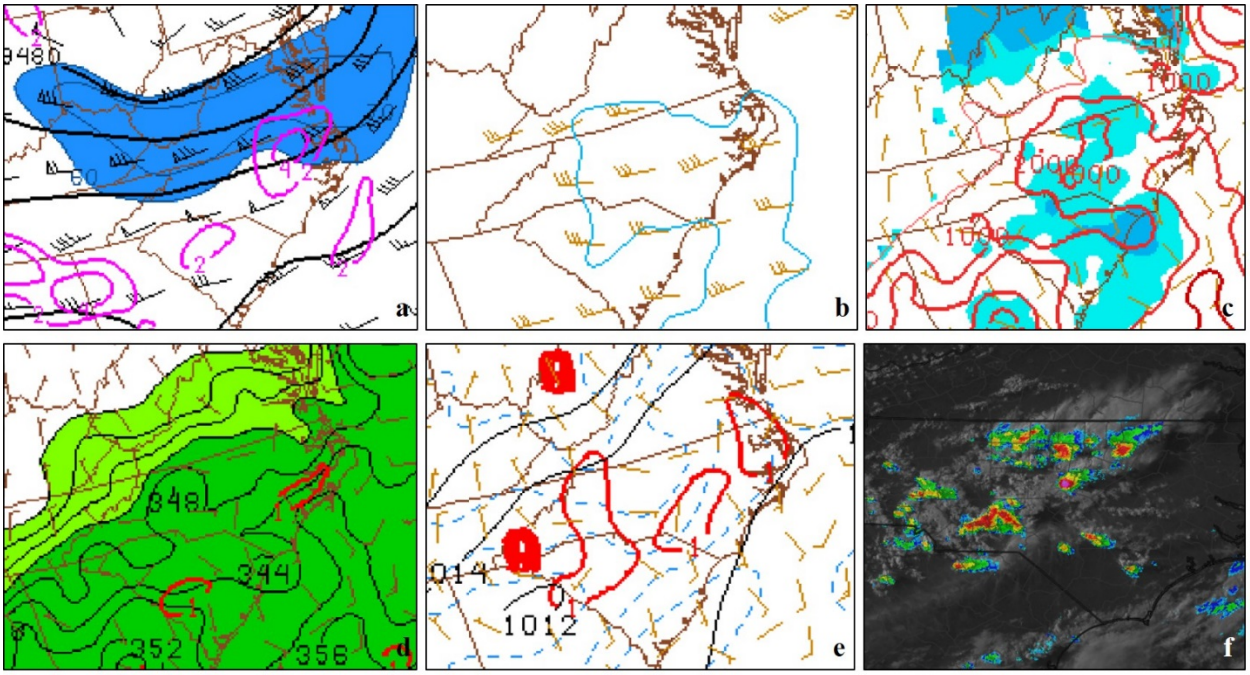

Figure 5. (a) NOAA/SPC HMAA 300 hPa height/divergence/wind, (b) EBS in kts, (c) SBCAPE (contoured) and SB convective inhibition (SBCIN), shaded, at 25 and 100 J kg^{-2}, (d) surface θ_e/advection in K per hour, (e) surface frontogenesis/temperature/pressure/wind (f) and IEM base reflectivity/visible satellite imagery, at 23 UTC on 29 June 2016.

e. Type B surface boundaries

Type B surface boundaries included weak/decaying quasi-stationary surface frontal boundaries that stretched from west to east across SHZDC. These boundaries helped initiate convection on 12 forecast low probability SWAP days. In many instances, these boundaries were so weak that they were difficult to find, even using surface sea level pressure (SLP). Nevertheless, the general surface wind and SLP patterns can be distinguished (Figs. 6a,b). During 9 of these 12 Type B boundary-influenced SWAP days, sea-breeze boundaries interacted with Type B boundaries to increase convection. PTs detected near Type B boundaries on 7 of the 12 Type B boundary-influenced SWAP days also enhanced convective development. Weak lee lows appeared to increase convection near Type B boundaries on five forecast low probability Type B-influenced SWAP days. Surface frontogenesis occurred where convection developed on 10 of the 12 Type B boundary-influenced SWAP days.

The atmosphere across SHZDC on Type B boundary-influenced SWAP days was unstable, with SBCAPE values of at least 1000 kg m^{-2} prior to/during convective development on all 12 days, while EBS values at or greater than 25 kts helped organized convection (Thompson et al. 2003) on 8 days. Like the Type A-enhanced convection, though, not all convection propagated in the direction of the EBS vectors. On 11 Type B boundary-influenced SWAP days, surface θ_e values of at least 340 K were observed; values reached at least 356 K during 7 Type B boundary-influenced SWAP days.

Convection developed underneath areas of 300 hPa divergence during all 12 Type B

boundary-influenced SWAP days. On 9 of the 12 days, convection initiated below the right entrance region of a 300 hPa jet maximum, while convection developed beneath the left exit region of a 300 hPa jet maximum on just 1 of the 12 days. Mid-level short-wave troughs boosted convective potential during all 12 Type B boundary-influenced SWAP days. These short-wave troughs seemed to work in concert with both upper-level divergence/jet maxima and Type B/other mesoscale surface boundaries to instigate/sustain convection. Figure 6c illustrates the convective precipitation pattern across SHZDC on Type B boundary-influenced SWAP days.

A review of 12 UTC LAMP convection probability forecasts revealed that using a minimum value of 30% may have increased forecaster confidence on 6 of the 12 (50% of) Type B boundary-enhanced SWAP days. During those 6 days, the LAMP 30% convection probability threshold was reached within 1-2 hours of observed convective initiation, then crossed below that threshold within 1-2 hours of observed convective dissipation. Areal coverage was generally good throughout the 6 useful LAMP 30% convection probability forecasts, but, again, there were times when the areal extent was off by more than 50 miles in at least one direction when compared to where convection formed/tracked. The poorer performance of LAMP convection probability forecasts prior to Type B-enhanced SWAP events may be due to the LAMP having difficulties resolving and forecasting the weak/decaying quasi-stationary surface boundaries.

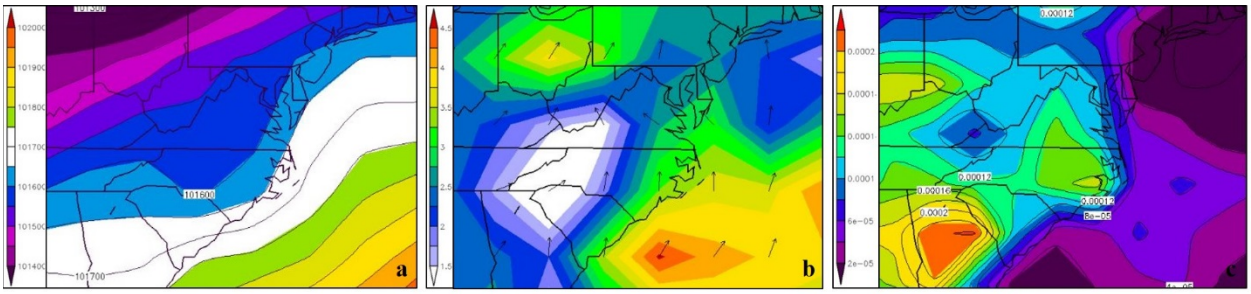

Figure 6. (a) Six-hour NCEP/NCAR reanalysis data composite images of surface sea level pressure in Pa at 18 UTC, (b) surface vector wind at 18 UTC, and (c) surface convective precipitation rate in mm per day averaged from 18 UTC to 00 UTC, for all Type B-enhanced SWAP days in this study. Data are courtesy of NOAA/ESRL.

f. Type B surface boundaries example: 18-19 June 2015

Convection initially developed ahead of mid-level short-wave troughs and along a few different east-west oriented quasi-stationary surface boundaries across SHZDC around 1830 UTC on 18 June 2015. Over the next few hours, convection organized into two west-east oriented broken lines, with more convection developing 2200 UTC along colliding outflow boundaries produced by the two lines of convection. Convection slowly dissipated after 02 UTC on 19 June 2015. Per FAA Northeast Recap logs, jet routes across SHZDC were impacted for several hours as the SWAP included route closures and re-routes to avoid the convection. Figure 7 shows a "snapshot" of the Type B-enhanced convective SWAP

event at 00 UTC on 19 June 2015. Convection intensified under the right entrance region of an upper-level jet maximum (Fig. 7a), with EBS values ranging from less than 25 kts across North Carolina to 25-30 kts with eastward trajectories across southern Virginia (Fig. 7b). SBCAPE values were generally 1000-3000 kg m^{-2} (Fig. 7c) where convection formed. Convection developed in an area of high surface θ_e (Fig. 7d) within areas of weak surface frontogenesis across SHZDC (Fig. 7e). By 00 UTC on 19 June 2015, convective clusters were occurring with anvil cirrus extending several tens of kilometers northeastward from parent convection (Fig. 7f).

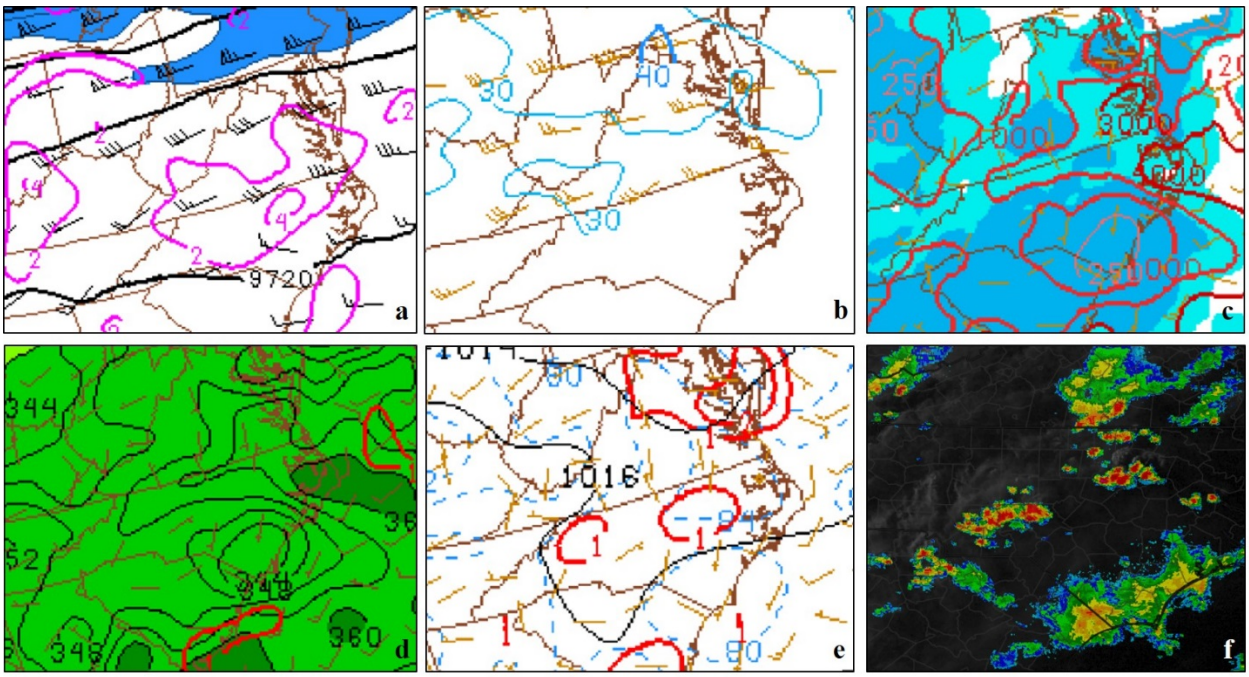

Figure 7. Same as Figure 5, except at 00 UTC on 19 June 2015.

4. Summary and Future Work

Under-forecast convection (i.e. when a low probability of a SWAP was forecast) across SHZDC caused the FAA to implement unanticipated SWAP initiatives on 30 days during the April to October timeframe in 2015, 2016 and 2017. Two types of synoptic-scale surface boundaries across SHZDC aided the SWAP-causing convective development and evolution. The first boundary type – Type A – comprised both surface cold fronts moving in a southward direction into or across SHZDC and west to east-oriented quasi-stationary fronts across SHZDC along which a surface wave or area of low pressure developed and tracked eastward, forcing part of the front southward. The second boundary type – Type B – consisted of weak quasi-stationary west to east-oriented surface frontal boundaries across SHZDC.

Interaction with mesoscale boundaries was important, as Type A and Type B boundaries collided with a sea-breeze front and/or a PT during 87% of the SWAP days. Several other environmental factors also assisted in convective development and evolution. These factors included upper-level divergence and transiting mid-level shortwaves during convective development/evolution on all of the SWAP

days, SBCAPE values at least 1000 J kg m^{-2} near Type A and Type B boundaries during the afternoon/evening on 97% of the SWAP days, surface θ_e values equal to or greater than 340K during 90% of the SWAP days and EBS values of 25 kts or greater near Type A and Type B boundaries on 73% of the SWAP days. Early morning LAMP convection forecasts yielded mixed results. LAMP convection forecasts had better success on Type A boundary-enhanced SWAP days than on Type B boundary-enhanced SWAP days. The poorer performance prior to the onset of convection on Type B boundary-enhanced SWAP days may be due to the LAMP not resolving weaker quasi-stationary surface boundaries well.

Future work to improve the accuracy of SWAP statements and other aviation-related convection forecast products across SHZDC may include a number of initiatives. One such initiative may be to create a null dataset to compare with the dataset used to create this TA. The null dataset could include cases when patterns discussed in this TA were evident, a low probability of a SWAP was forecast and convection did not develop to the point of requiring a SWAP. A second set of actions may be the development of pattern-based reference aids and decision trees highlighting the two types of synoptic-scale surface boundaries and other important environmental factors discussed in this TA. Finally, input into LAMP convection forecasts was changed in early 2018 (J. Ghirardelli, personal communication, 3 July 2018), so future studies of LAMP convection forecasts and future use of LAMP convection-related data to pinpoint areas most prone to a SWAP across SHZDC may yield improved results.

Acknowledgements

Thanks to Richard Winther, Meteorologist-In-Charge (MIC), NWS ZDC CWSU, Steven Zubrick, Science and Operations Officer, NWS Weather Forecast Office (WFO) Sterling, VA, James Lee, MIC, WFO Sterling, VA, Brian Miretzky and Dave Radell, NWS Eastern Region Scientific Services Division, and anonymous reviewers for providing helpful comments and feedback.

References

Cobb, S. 1995: A case study of a severe thunderstorm outbreak in southern Virginia. NWS ER Technical Attachment 95-3A.

Dirks, R. A., J. P. Kuettner, and J. A. Moore, 1988: Genesis of Atlantic Lows Experiment (GALE): An overview. *Bull. Amer. Meteor. Soc.,* **69,** 148-160.

Federal Aviation Administration (FAA) Daily Northeast Recap Logs. [Available from the FAA upon request.]

Ghirardelli, J. (3 July 2018). Personal correspondence.

Iowa Environmental Mesonet, 2013: IEM NEXRAD Composite Base Reflectivity Archive. [Available online at http://mesonet.agron.iastate.edu/GIS/apps/rview/warnings.phtml]

Koch, S. E. and C. A. Ray, 1997: Mesoanalysis of summertime convergence zones in central and eastern North Carolina. *Wea. Forecasting,* **12,** 56-77.

Mattocks, C. and R. Bleck, 1986: Jet streak dynamics and geostrophic adjustment processes during the initial stages of lee

cyclogenesis. *Mon. Wea. Rev.,* **114,** 2033-2056.

NOAA/Earth System Research Laboratory. Physical Sciences Division, 6-Hrly NCEP/NCAR Reanalysis Data Composites. [Available online at https://www.esrl.noaa.gov/psd/data/composites/hr/.]

NOAA/NWS Meteorological Development Lab LAMP Convection Image Repository. [Available online at https://sats.nws.noaa.gov/~glmp/conv_arc/index.php.]

NOAA/NWS National Centers for Environmental Prediction. Weather Prediction Center Surface Analysis Archive. [Available online at http://www.wpc.ncep.noaa.gov/archives/web_pages/sfc/sfc_archive.php.]

NOAA/NWS Storm Prediction Center Hourly Mesoscale Analysis Archive. [Available online at http://www.spc.noaa.gov/exper/ma_archive/.]

O'Handley, C., and L. F. Bosart, 1996: The impact of the Appalachian Mountains on cyclonic weather systems. Part I: A climatology. *Mon. Wea. Rev.,* **124,** 1353-1373.

Pfaff, S. R., 2002: A WSR-88D investigation of a non-characteristic severe thunderstorm over southeast North Carolina. NWS ER-Technical Attachment 2002-05.

Rose, S. F., P. V. Hobbs, J. D. Locatelli, and M. T. Stoelinga, 2004: A 10-yr climatology relating the locations of reported tornadoes to the quadrants of upper-level jet streaks. *Wea. Forecasting,* **19,** 301-309.

Squires, K. and K. Struckmann, 2009: Verification of Severe Weather Avoidance Plan (SWAP) forecasts for the New York Air Route Traffic Control Center (ARTCC) issued by the NWS Center Weather Service Unit (CWSU), Ronkonkoma, NY. NWS ER-Technical Attachment 2009-02.

Thompson, R. L., C. M. Mead, and R. Edwards, 2003: Effective storm-relative helicity and bulk shear in supercell thunderstorm environments. *Wea. Forecasting,* **22**, 102-115.

Vescio, M. D., K. K. Keeter, G. Dial, O. Badgett, and A. J. Riordan, 1993: A low-top weak reflectivity severe weather episode along a thermal/moisture boundary in eastern North Carolina, Pre-prints, *17th Conf. on Severe Local Storms*, St. Louis, MO, *Amer. Meteor. Soc.*, 629-633.

Weiss, J., 2014: Analysis of a left moving supercell that produced giant hail across northeast South Carolina. NWS ER-Technical Attachment 2014-02.